Electronic Supplementary Material (ESI) for Journal of Materials Chemistry C.

Supporting Information

Synthesis and characterization of azobenzene molecular glasses with different glass transition temperatures

Austin Diggins[a], Eoin Dawson[a], Mahnaz Kamaliardakani[b], Christian Pellerin[b], Ribal Georges Sabat[a] and Olivier Lebel[c]

[a] Department of Physics and Space Science, Royal Military College of Canada, PO Box 17000, Station Forces Kingston, Ontario CANADA, K7K 7B4

[b] Département de chimie, Université de Montréal, C.P. 6128, succursale Centre-ville, Montréal, Québec, CANADA, H3C 3J7

[c] Department of Chemistry and Chemical Engineering, Royal Military College of Canada, PO Box 17000, Station Forces Kingston, Ontario CANADA, K7K 7B4

[*]Corresponding author: c.pellerin@umontreal.ca, sabat@rmc.ca, Olivier.Lebel@rmc.ca

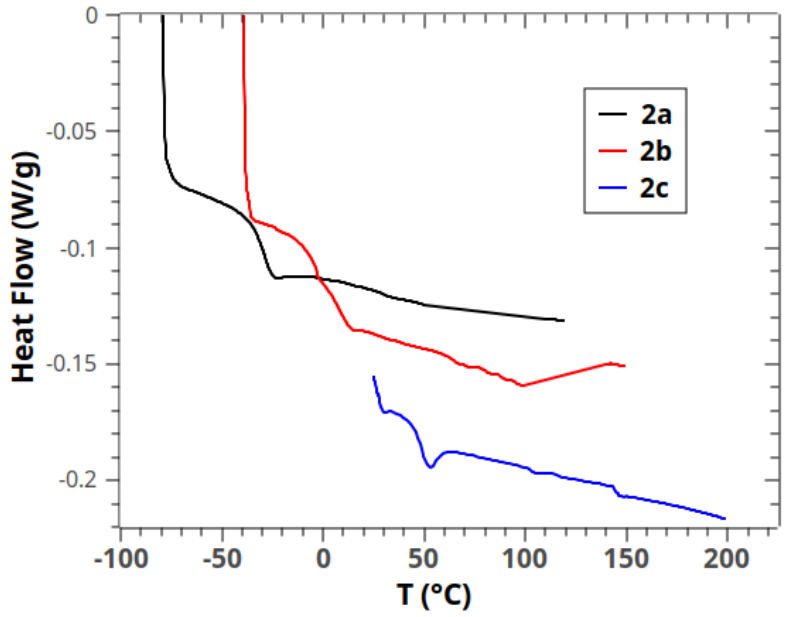

Figure S1. DSC thermograms of precursors **2a-c**. The thermograms were recorded at a heating rate of 5 °C/min after a preliminary heating run to erase the thermal history. Exotherms are facing up.

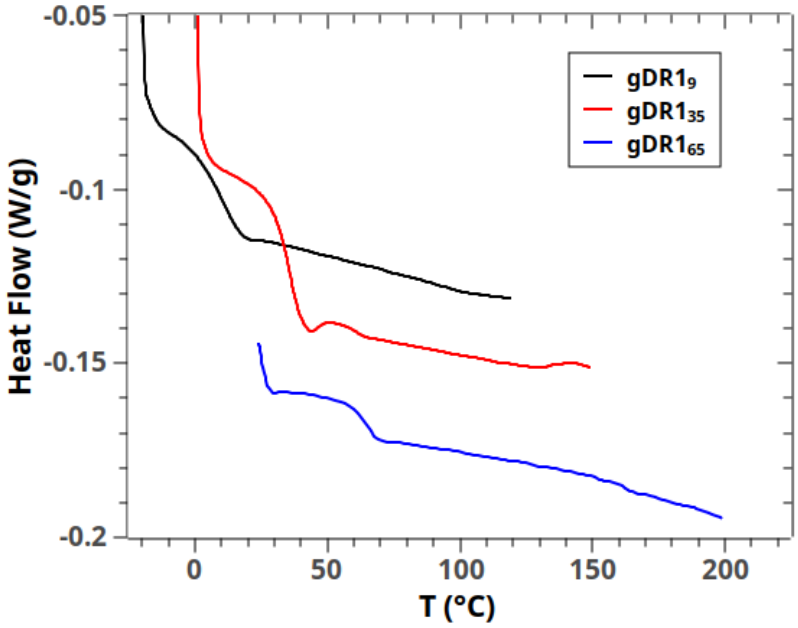

Figure S2. DSC thermograms of **gDR1$_9$**, **gDR1$_{35}$** and **gDR1$_{65}$**. The thermograms were recorded at a heating rate of 5 °C/min after a preliminary heating run to erase the thermal history. Exotherms are facing up.

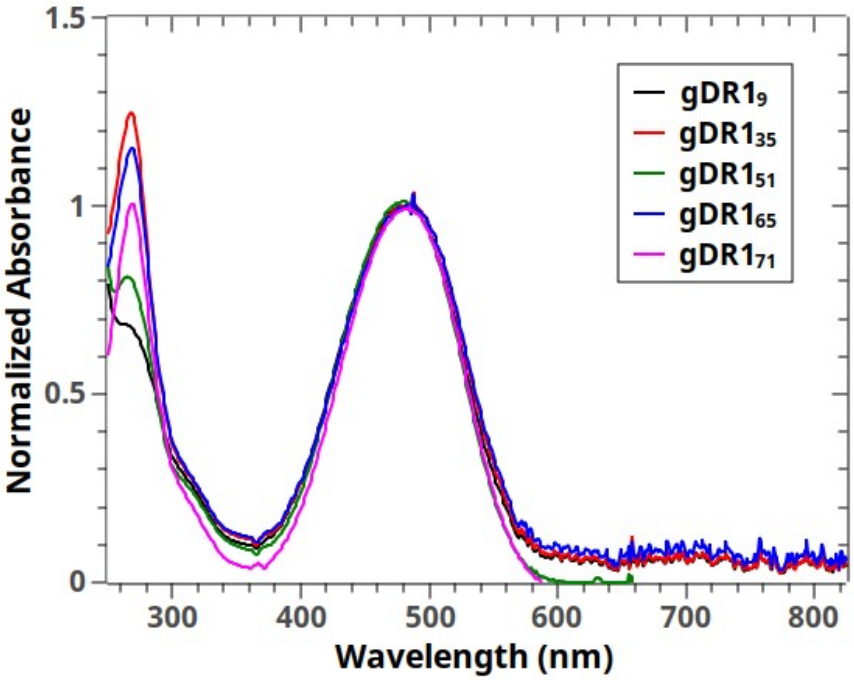

Figure S3. Normalized UV-Visible spectra of the different **gDR1$_{Tg}$** analogues used in the present study. Spectra were recorded in 0.01 mM solution in CH_2Cl_2.

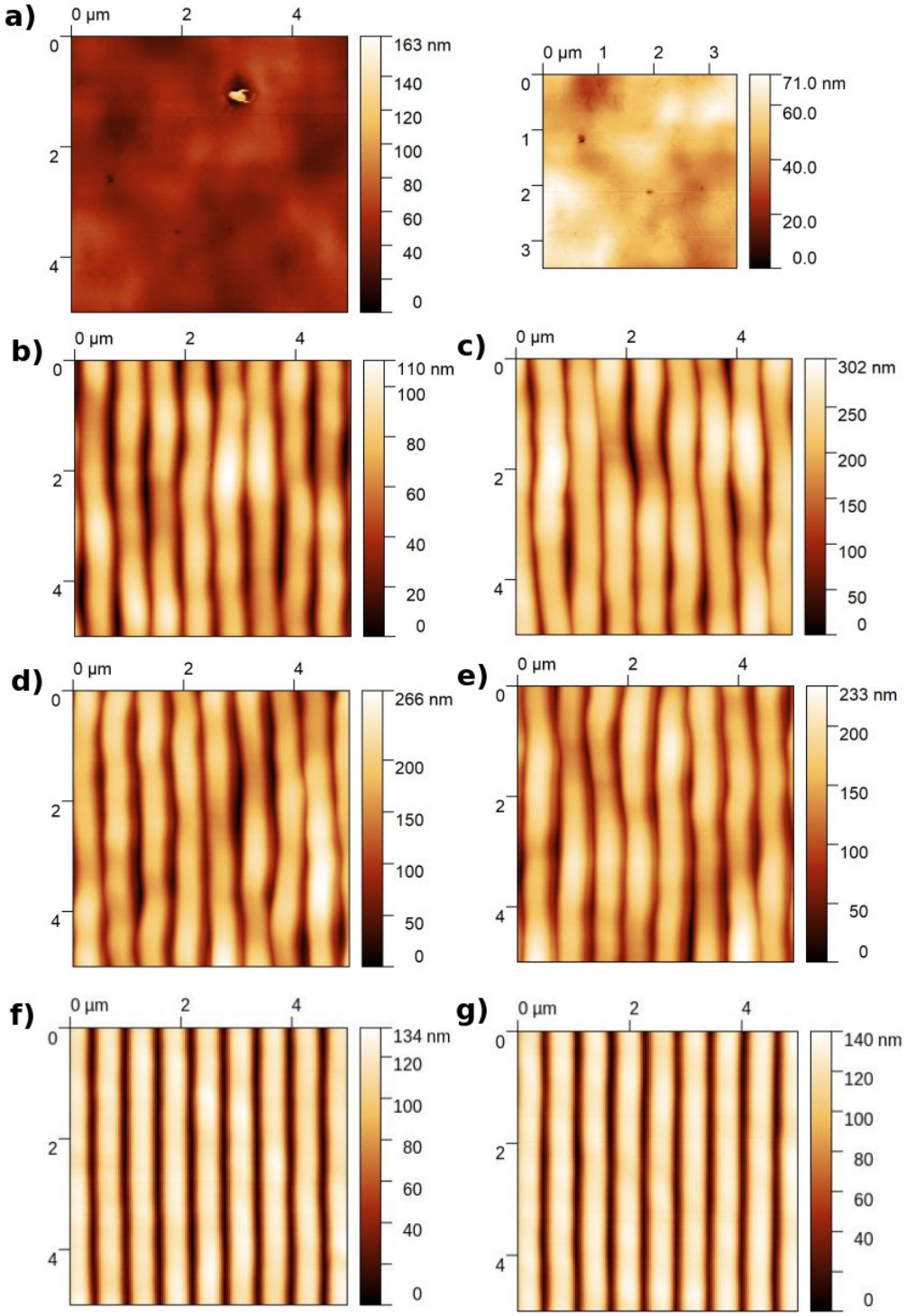

Figure S4. Atomic Force Microscopy (AFM) scans of thin films of **gDR1$_{Tg}$** after irradiation with a 488 nm laser at an irradiance of 100 mW/cm^2. (a) **gDR1$_9$** after 200 s irradiation; (b) **gDR1$_{35}$** after 200 s irradiation; (c) **gDR1$_{51}$** after 600 s irradiation; (d) **gDR1$_{65}$** after 600 s irradiation; (e) **gDR1$_{71}$** after 800 s irradiation; (f) **gDR1$_{65}$** after 60 irradiation (at 300 mW/cm^2); (g) **gDR1$_{71}$** after 150 s irradiation. The AFM scan for **gDR1$_9$** was recorded 2 h after irradiation was stopped. A cropped image where the surface defect is not shown is also included for (a). The images in (b)-(e) likely show a distortion of the gratings due to the longer irradiation times, as the gratings shown in images (f)-(g), which had not yet reached saturation, do not show such defects.

Table S1. Initial SRG inscription rates for **gDR1$_{Tg}$** with a 488-nm laser, obtained from the linear regression of the DE plots in Figure 1, before they plateaued.

Compound	Irradiance (mW/cm^2)	Inscription rate (DE %/s)	
gDR1$_9$	100	0.01226	$\pm 8 \times 10^{-5}$
	200	0.0248	$\pm 2 \times 10^{-4}$
	300	0.0338	$\pm 8 \times 10^{-4}$
gDR1$_{35}$	100	0.01514	$\pm 5 \times 10^{-5}$
	200	0.0405	$\pm 2 \times 10^{-4}$
	300	0.044	$\pm 1 \times 10^{-3}$
gDR1$_{51}$	100	0.0680	$\pm 1 \times 10^{-4}$
	200	0.1417	$\pm 6 \times 10^{-4}$
	300	0.0752	$\pm 7 \times 10^{-4}$
gDR1$_{65}$	100	0.0666	$\pm 1 \times 10^{-4}$
	200	0.1395	$\pm 5 \times 10^{-4}$
	300	0.151	$\pm 1 \times 10^{-3}$
gDR1$_{71}$	100	0.0575	$\pm 1 \times 10^{-4}$
	200	0.1149	$\pm 3 \times 10^{-4}$
	300	0.202	$\pm 1 \times 10^{-3}$

Table S2. Initial SRG inscription rates for **gDR1$_{Tg}$** with a 532-nm laser, obtained from the linear regression of the DE plots in Figure 1, before they plateaued.

Compound	Irradiance (mW/cm^2)	Inscription rate (DE %/s)	
gDR1$_9$	100	0.00272	$\pm 2 \times 10^{-5}$
	200	0.00175	$\pm 5 \times 10^{-5}$
	300	0.0112	$\pm 1 \times 10^{-4}$
gDR1$_{35}$	100	0.01279	$\pm 3 \times 10^{-5}$
	200	0.0298	$\pm 2 \times 10^{-4}$
	300	0.02655	$\pm 9 \times 10^{-5}$
gDR1$_{51}$	100	0.0532	$\pm 1 \times 10^{-4}$
	200	0.0748	$\pm 3 \times 10^{-4}$
	300	0.0708	$\pm 2 \times 10^{-4}$
gDR1$_{65}$	100	0.05366	$\pm 6 \times 10^{-5}$
	200	0.0926	$\pm 3 \times 10^{-4}$
	300	0.092	$\pm 3 \times 10^{-3}$
gDR1$_{71}$	100	0.05014	$\pm 7 \times 10^{-5}$
	200	0.0846	$\pm 2 \times 10^{-4}$
	300	0.0762	$\pm 2 \times 10^{-4}$

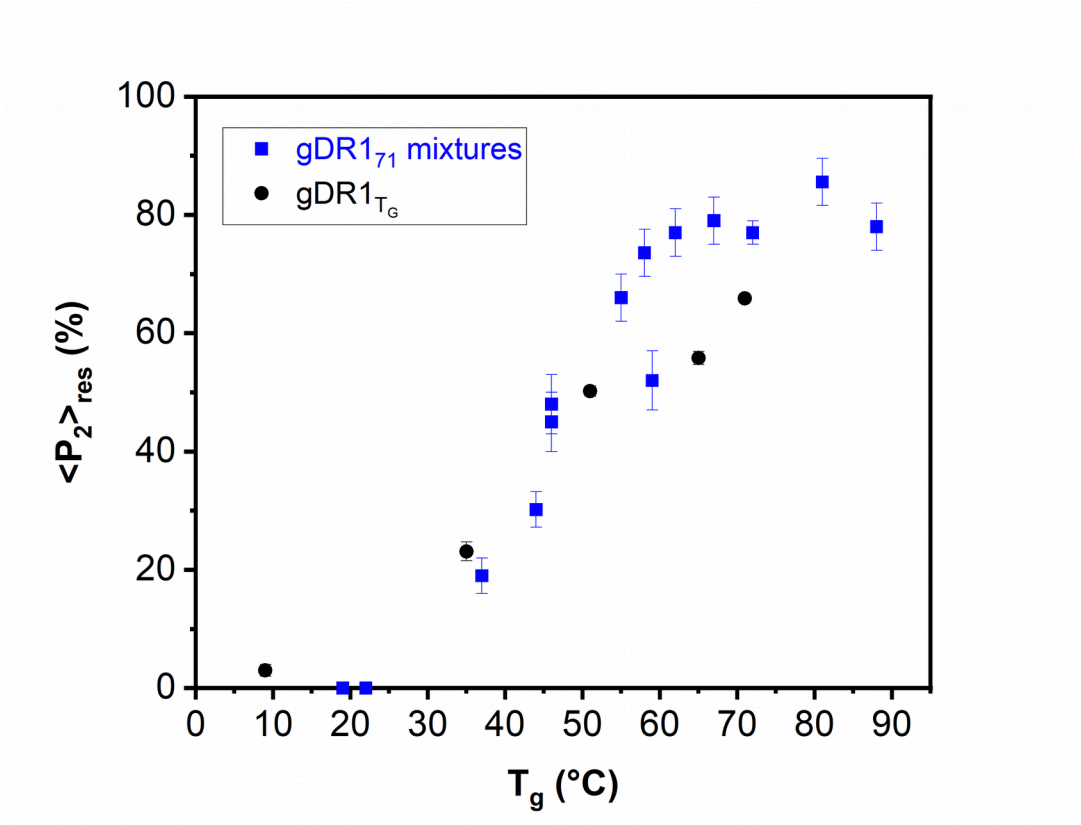

Figure S5. Effect of the glass transition temperature (T_g) on the residual orientation parameter ($<P_2>_{res}$) for pure $gDR1_{Tg}$ azo glasses (black) and for mixtures of azo glass $gDR1_{71}$ with photopassive glasses (blue). Similar trends are found for both cases. The mixtures results are reproduced from Ref. 24.

NMR Spectra of Compounds 1a-c, 2a-c, $gDR1_9$, $gDR1_{35}$ and $gDR1_{65}$

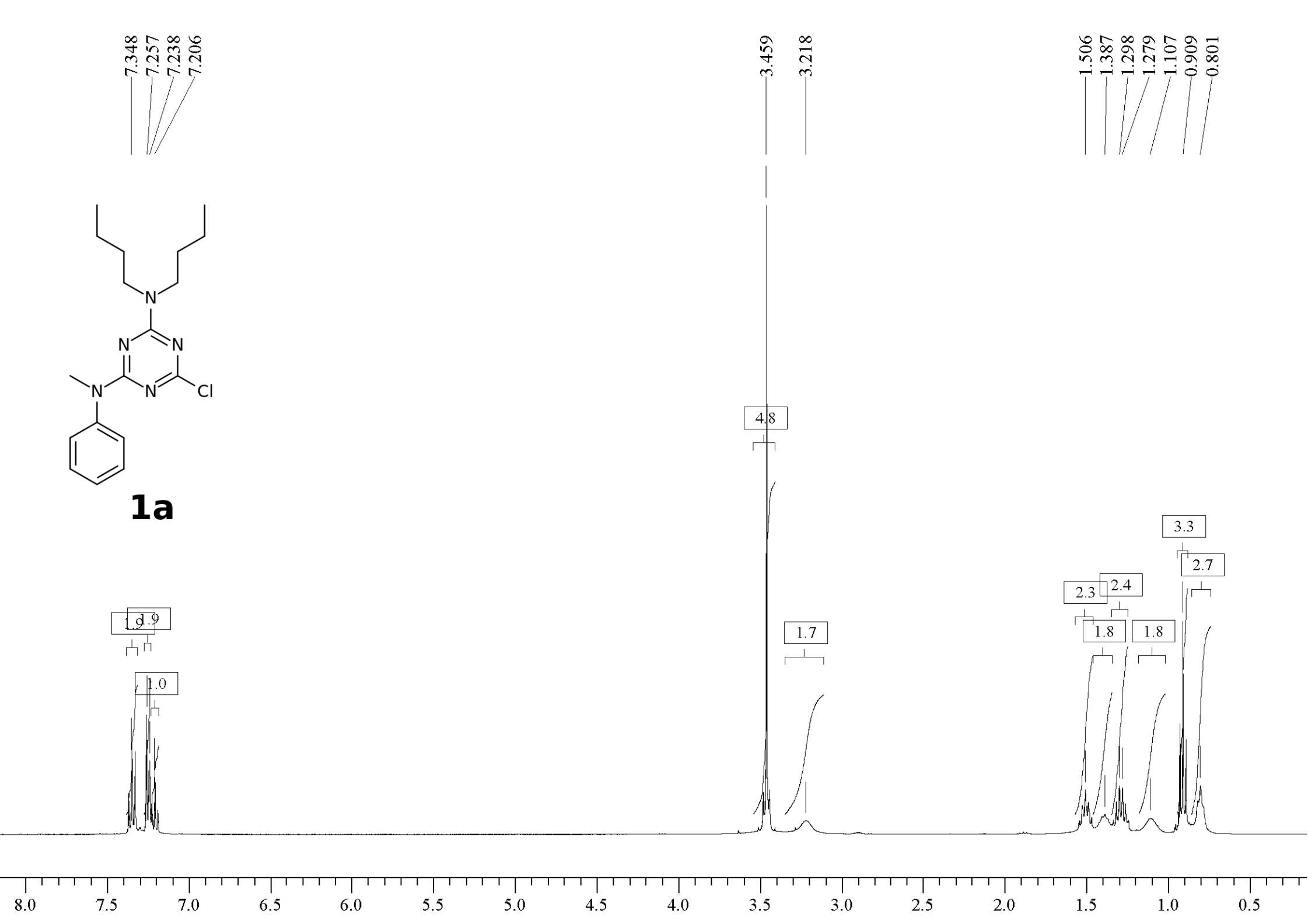
7.348
7.257
7.238
7.206
3.459
3.218
1.506
1.387
1.298
1.279
1.107
0.909
0.801
N
N
N
N
Cl
1a
4.8
1.7
1.9
1.9
1.0
3.3
2.7
2.3
2.4
1.8
1.8
8.0
7.5
7.0
6.5
6.0
5.5
5.0
4.5
4.0
3.5
3.0
2.5
2.0
1.5
1.0
0.5

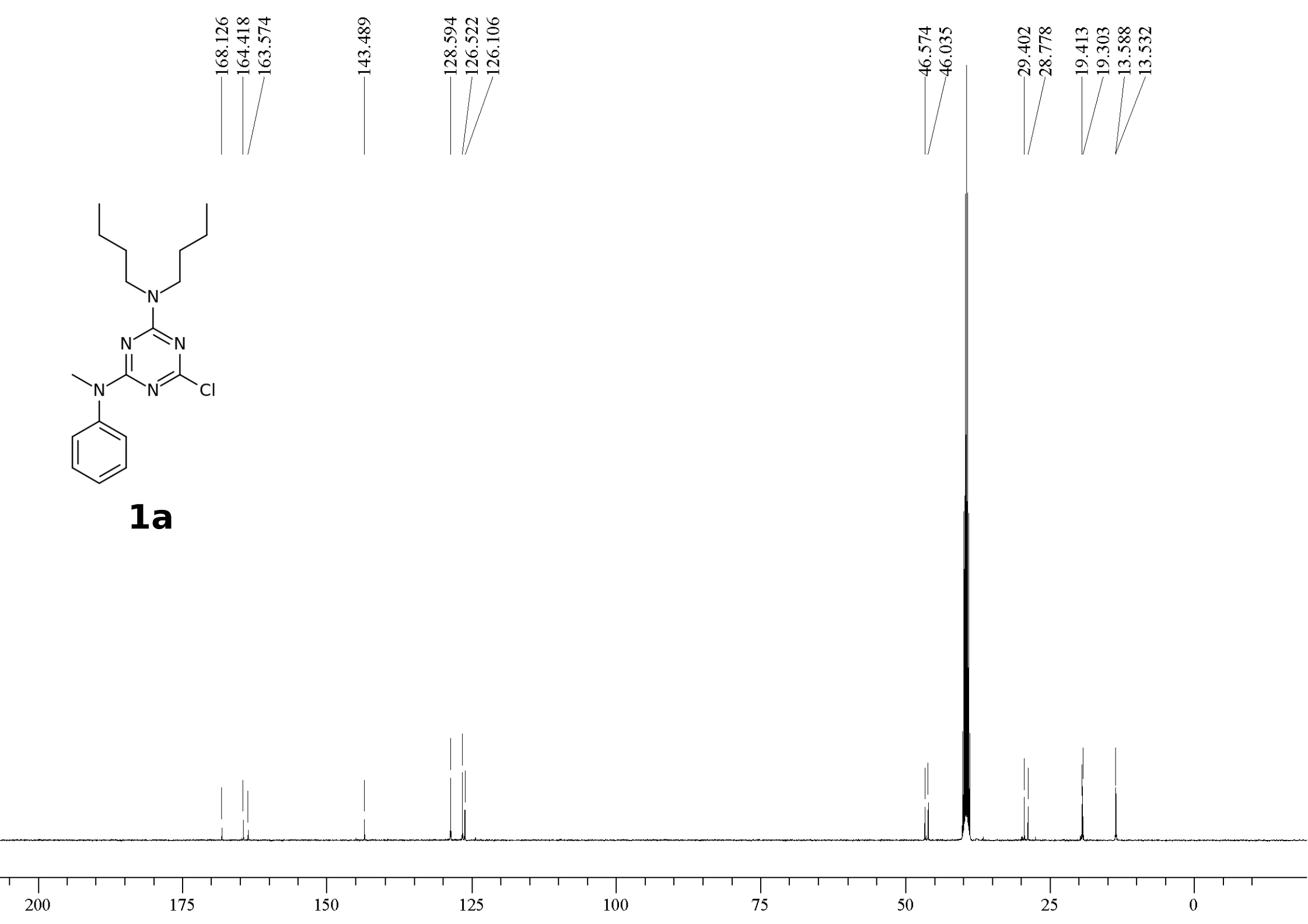
168.126
164.418
163.574
143.489
128.594
126.522
126.106
46.574
46.035
29.402
28.778
19.413
19.303
13.588
13.532
N
N
N
N
N
Cl
1a
200
175
150
125
100
75
50
25
0

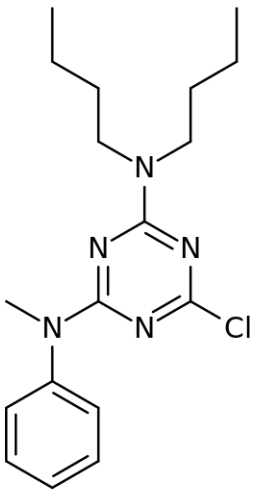

1a

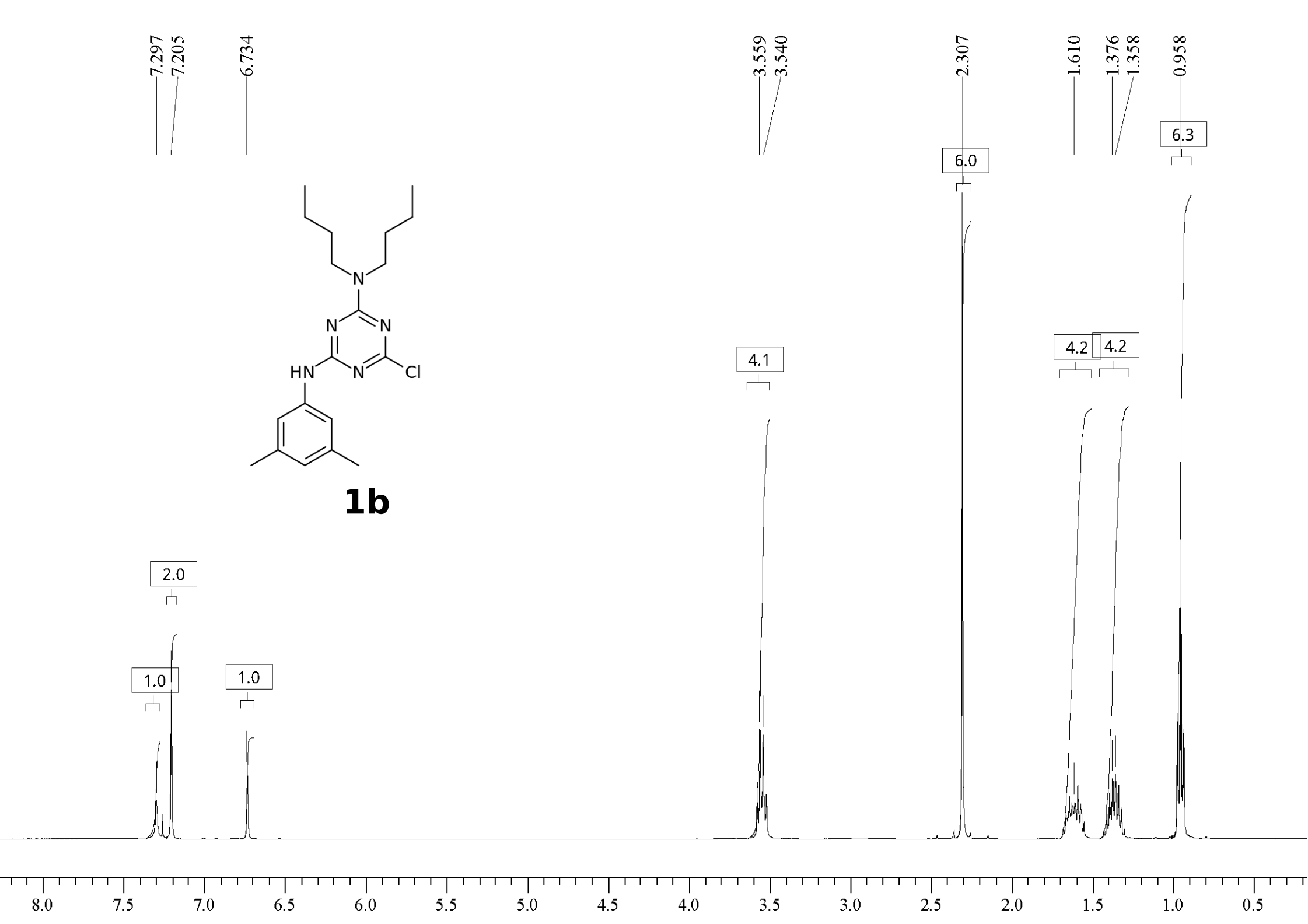
7.297
7.205
6.734
3.559
3.540
2.307
1.610
1.376
1.358
0.958
6.3
6.0
4.1
4.2
4.2
2.0
1.0
1.0
N
N
N
HN
N
Cl
1b
8.0
7.5
7.0
6.5
6.0
5.5
5.0
4.5
4.0
3.5
3.0
2.5
2.0
1.5
1.0
0.5

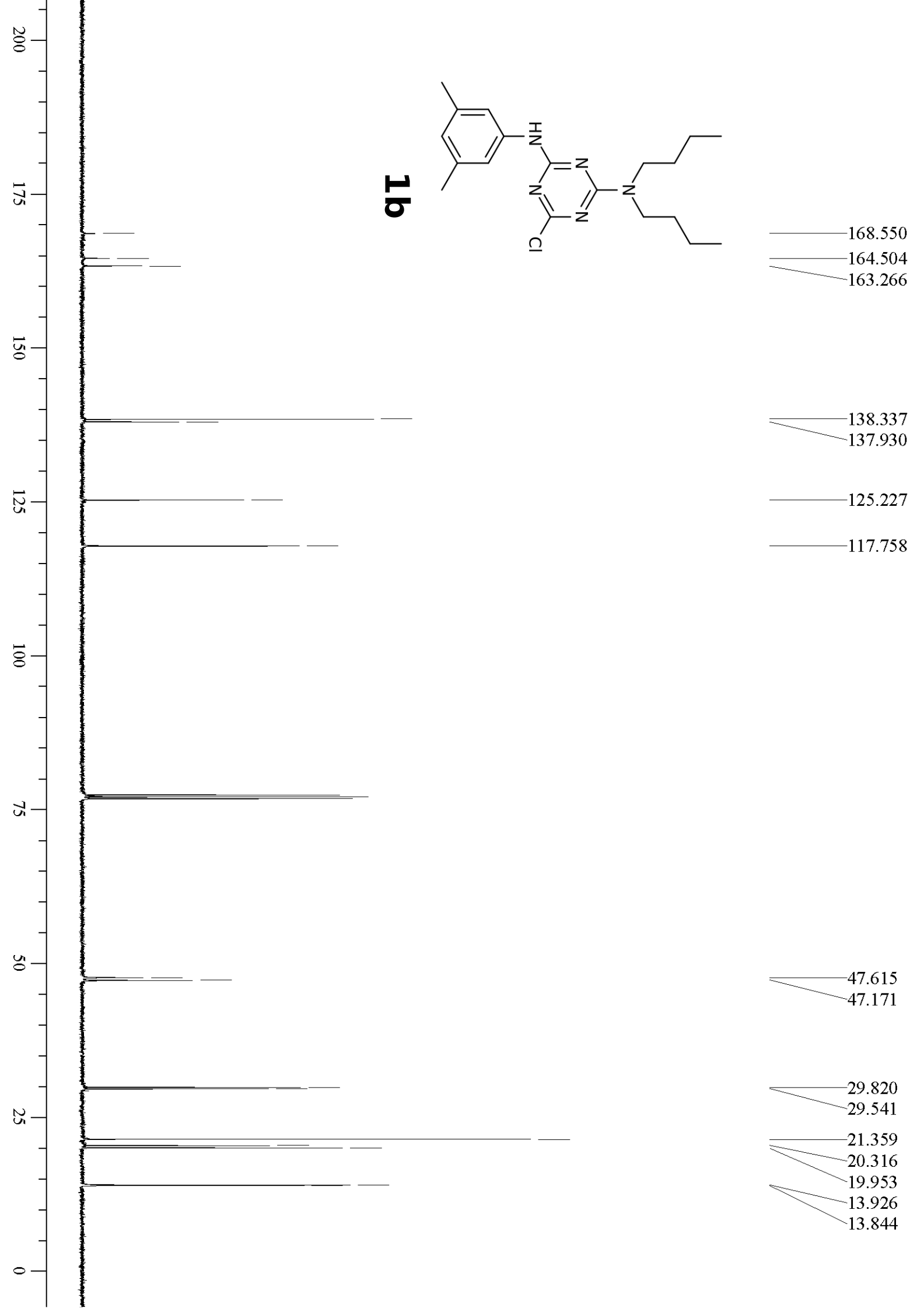
1b
HN
N
N
N
N
Cl
168.550
164.504
163.266
138.337
137.930
125.227
117.758
47.615
47.171
29.820
29.541
21.359
20.316
19.953
13.926
13.844
200
175
150
125
100
75
50
25
0

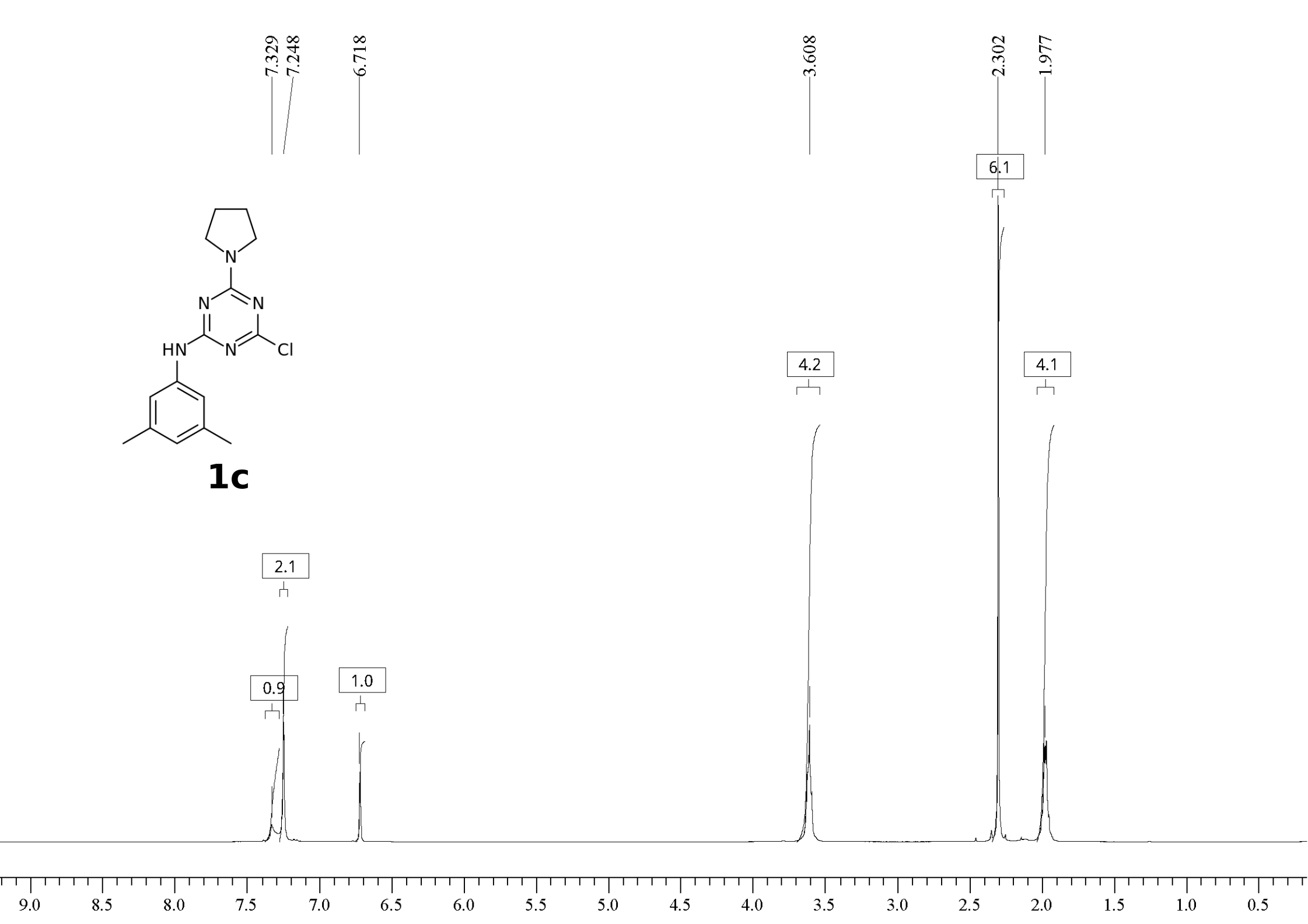
7.329
7.248
6.718
3.608
2.302
1.977
6.1
4.2
4.1
2.1
0.9
1.0
N
N
N
HN
N
Cl
1c
9.0
8.5
8.0
7.5
7.0
6.5
6.0
5.5
5.0
4.5
4.0
3.5
3.0
2.5
2.0
1.5
1.0
0.5

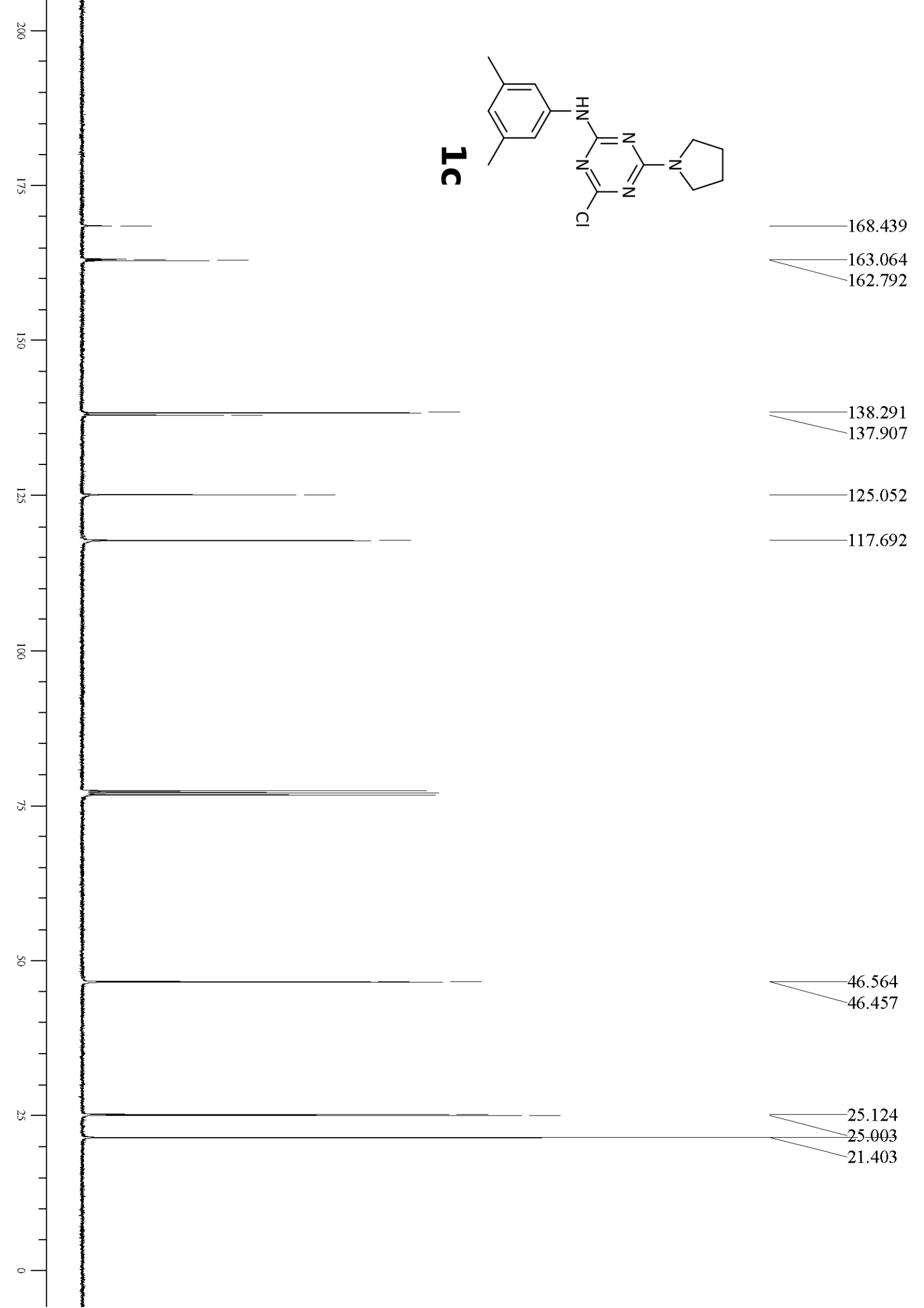
1c
HN
N
N
N
N
Cl
168.439
163.064
162.792
138.291
137.907
125.052
117.692
46.564
46.457
25.124
25.003
21.403
200
175
150
125
100
75
50
25
0

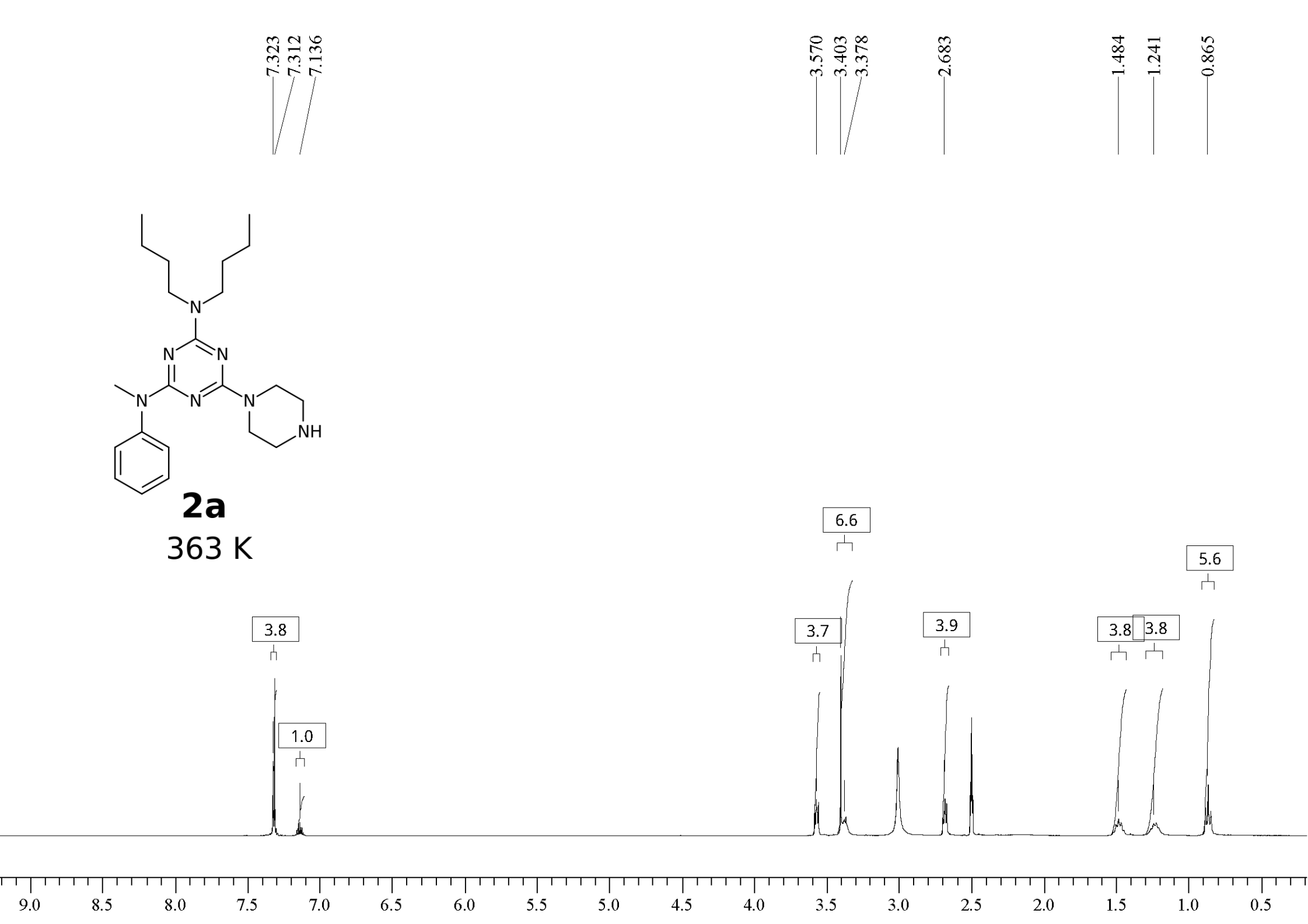
7.323
7.312
7.136
3.570
3.403
3.378
2.683
1.484
1.241
0.865
N
N
N
N
N
N
NH
2a
363 K
3.8
1.0
6.6
3.7
3.9
3.8
3.8
5.6
9.0
8.5
8.0
7.5
7.0
6.5
6.0
5.5
5.0
4.5
4.0
3.5
3.0
2.5
2.0
1.5
1.0
0.5

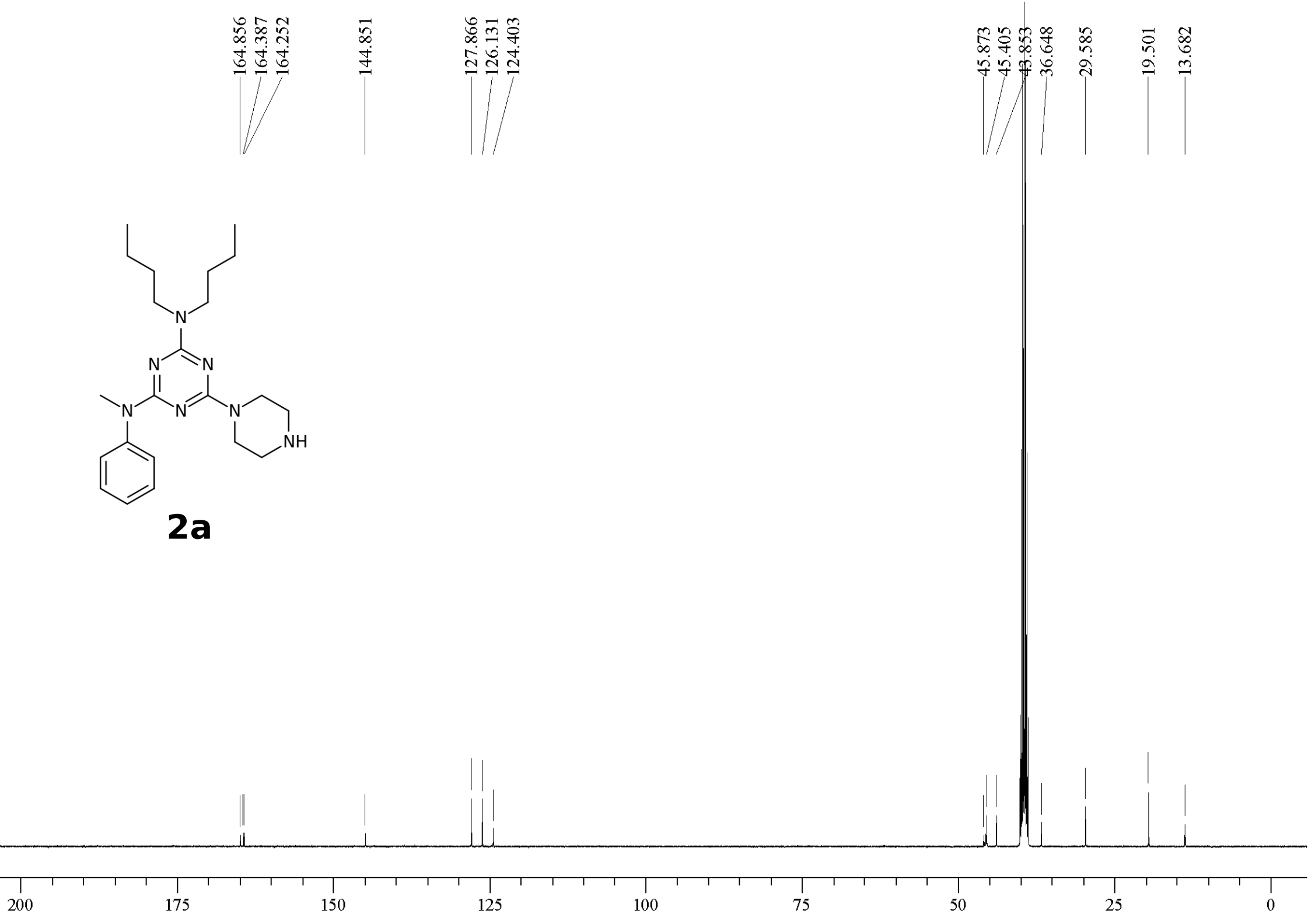
164.856
164.387
164.252
144.851
127.866
126.131
124.403
45.873
45.405
43.853
36.648
29.585
19.501
13.682
N
N
N
N
N
N
NH
2a
200
175
150
125
100
75
50
25
0

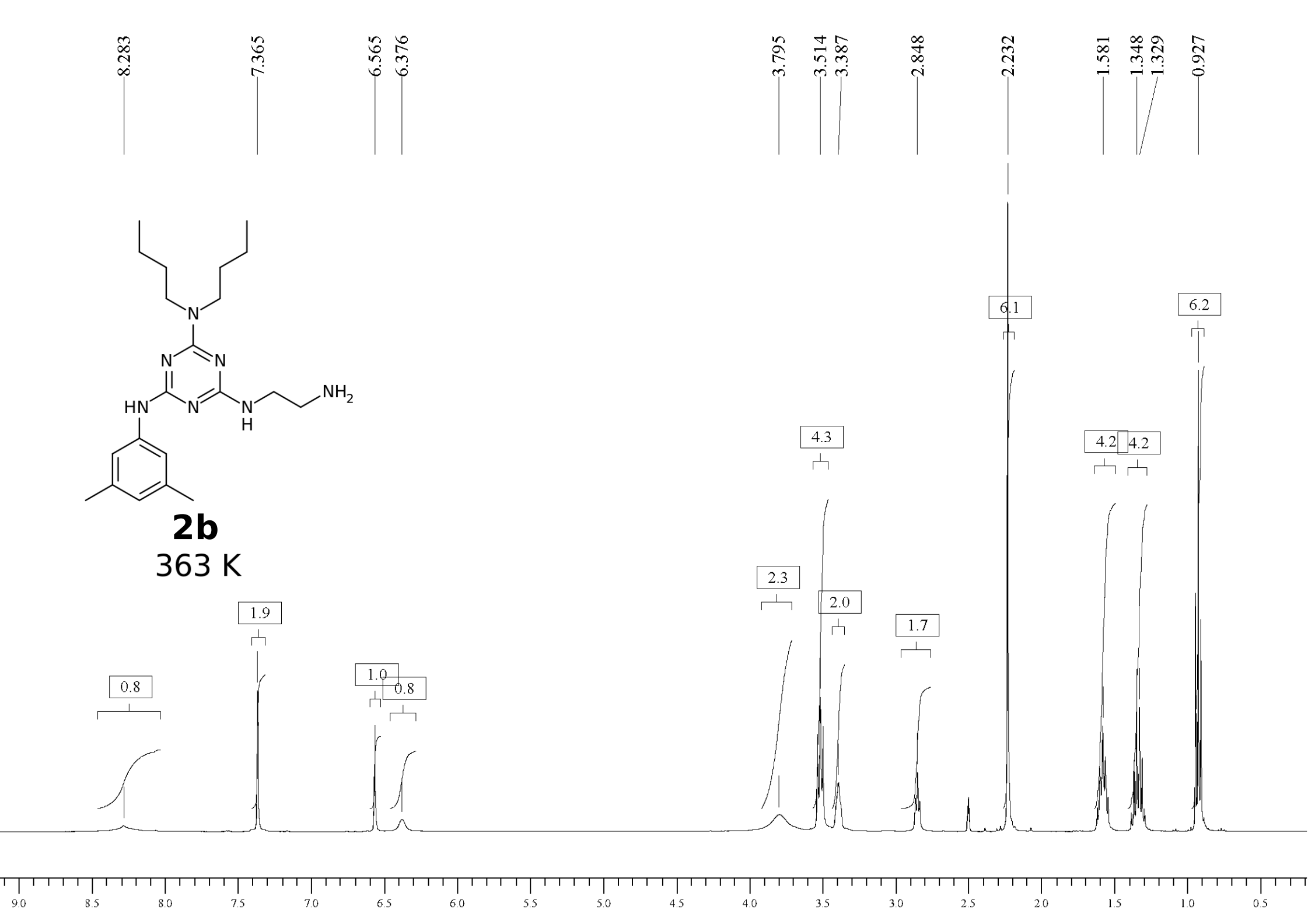
8.283
7.365
6.565
6.376
3.795
3.514
3.387
2.848
2.232
1.581
1.348
1.329
0.927
HN
N
N
N
N
N
H
NH2
2b
363 K
0.8
1.9
1.0
0.8
2.3
4.3
2.0
1.7
6.1
4.2
4.2
6.2
9.0
8.5
8.0
7.5
7.0
6.5
6.0
5.5
5.0
4.5
4.0
3.5
3.0
2.5
2.0
1.5
1.0
0.5

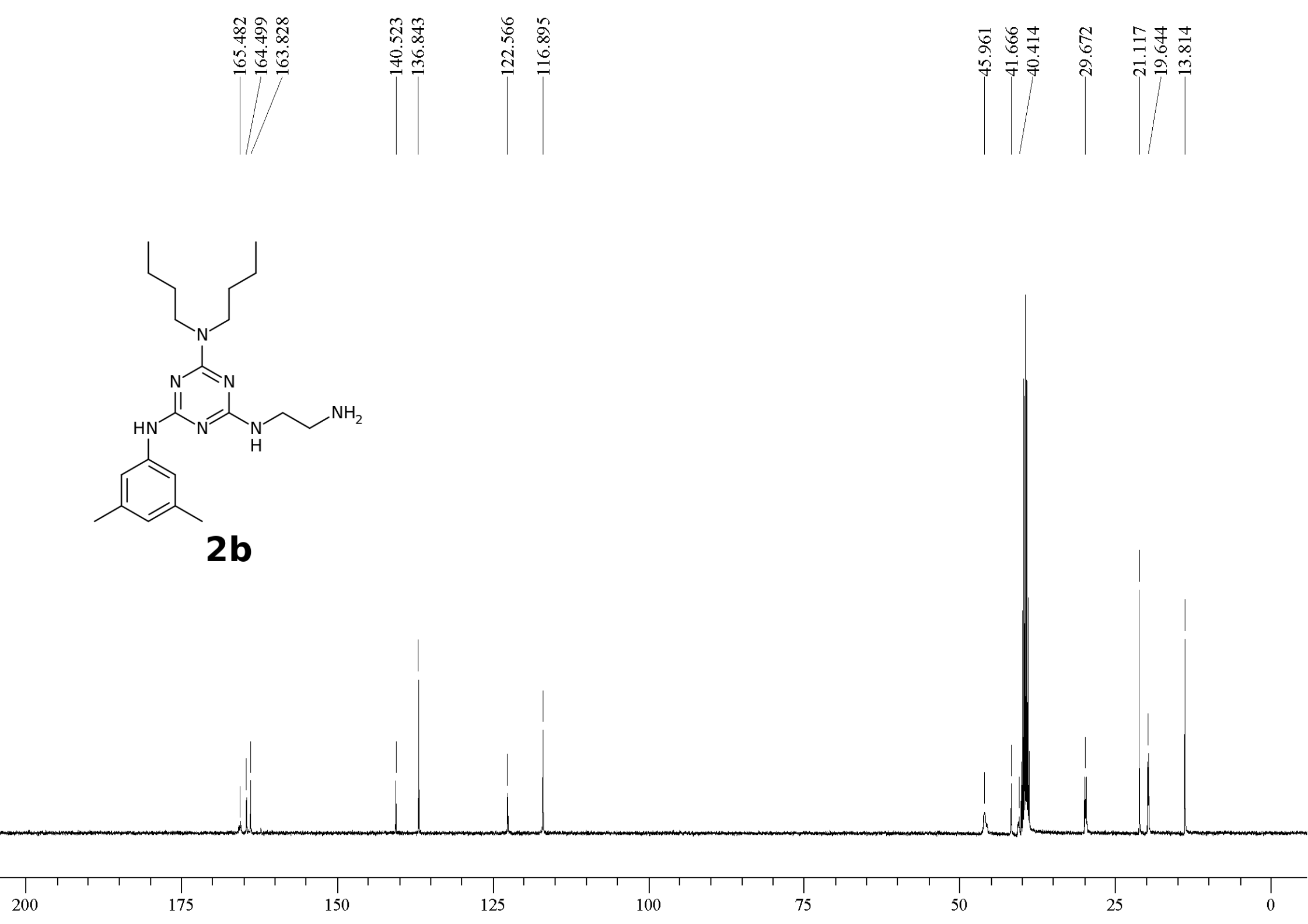
165.482
164.499
163.828
140.523
136.843
122.566
116.895
45.961
41.666
40.414
29.672
21.117
19.644
13.814
N
N
N
HN
N
N
H
NH2
2b
200
175
150
125
100
75
50
25
0

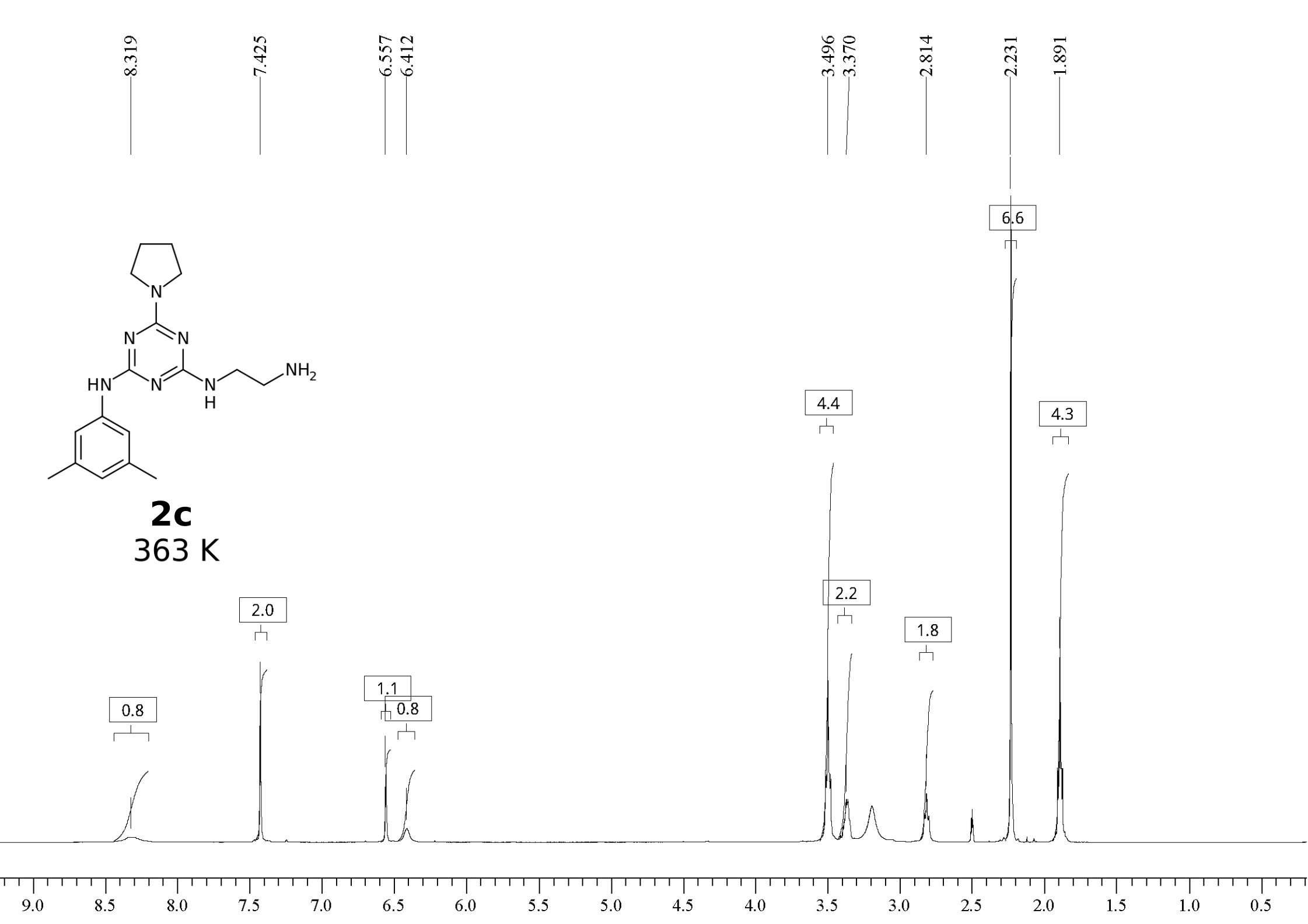
8.319
7.425
6.557
6.412
3.496
3.370
2.814
2.231
1.891
6.6
4.4
4.3
2.2
2.0
1.8
1.1
0.8
0.8
HN
N
N
N
N
H
NH2
2c
363 K
9.0
8.5
8.0
7.5
7.0
6.5
6.0
5.5
5.0
4.5
4.0
3.5
3.0
2.5
2.0
1.5
1.0
0.5

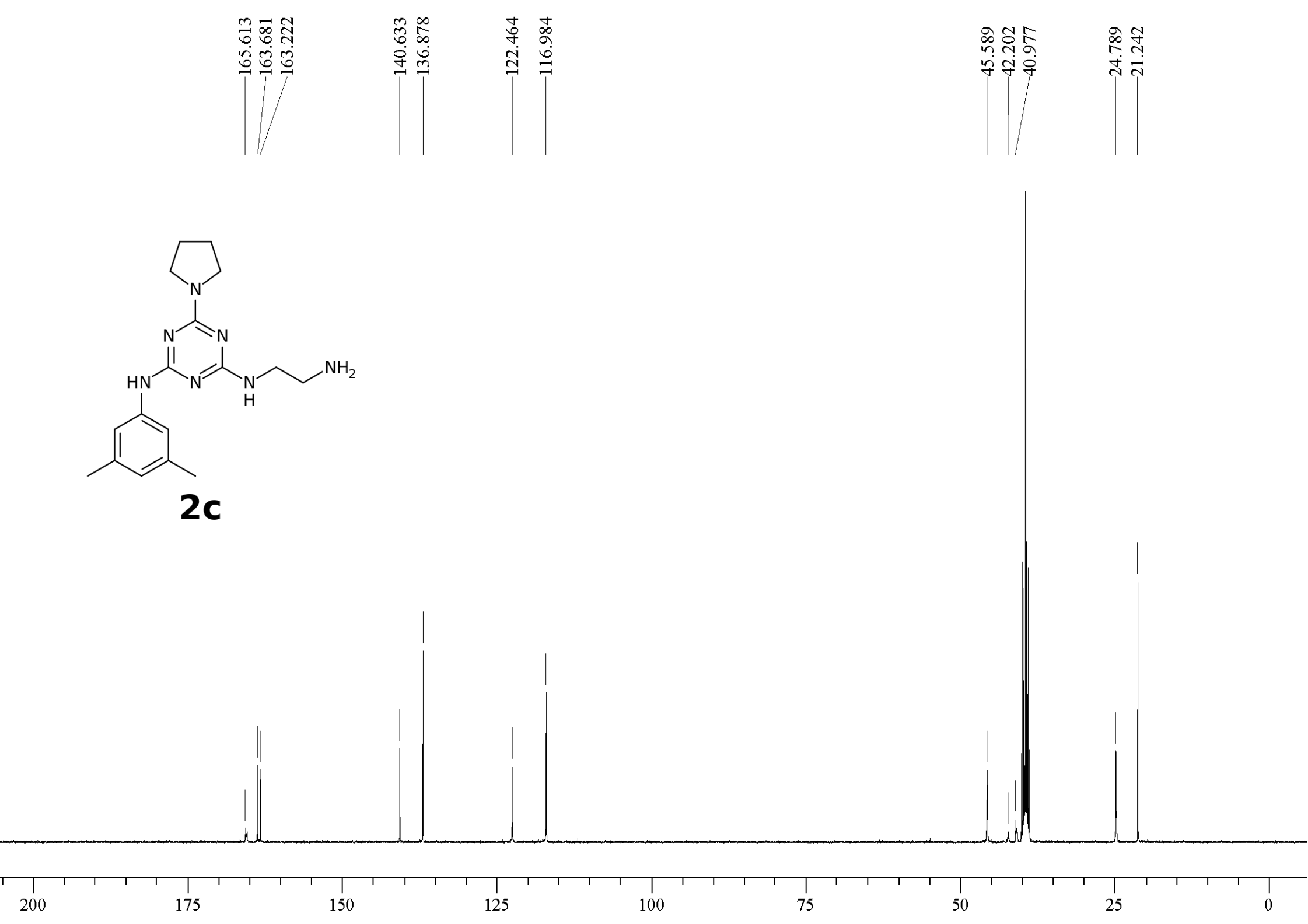
165.613
163.681
163.222
140.633
136.878
122.464
116.984
45.589
42.202
40.977
24.789
21.242
HN
N
N
N
N
H
NH2
2c
200
175
150
125
100
75
50
25
0

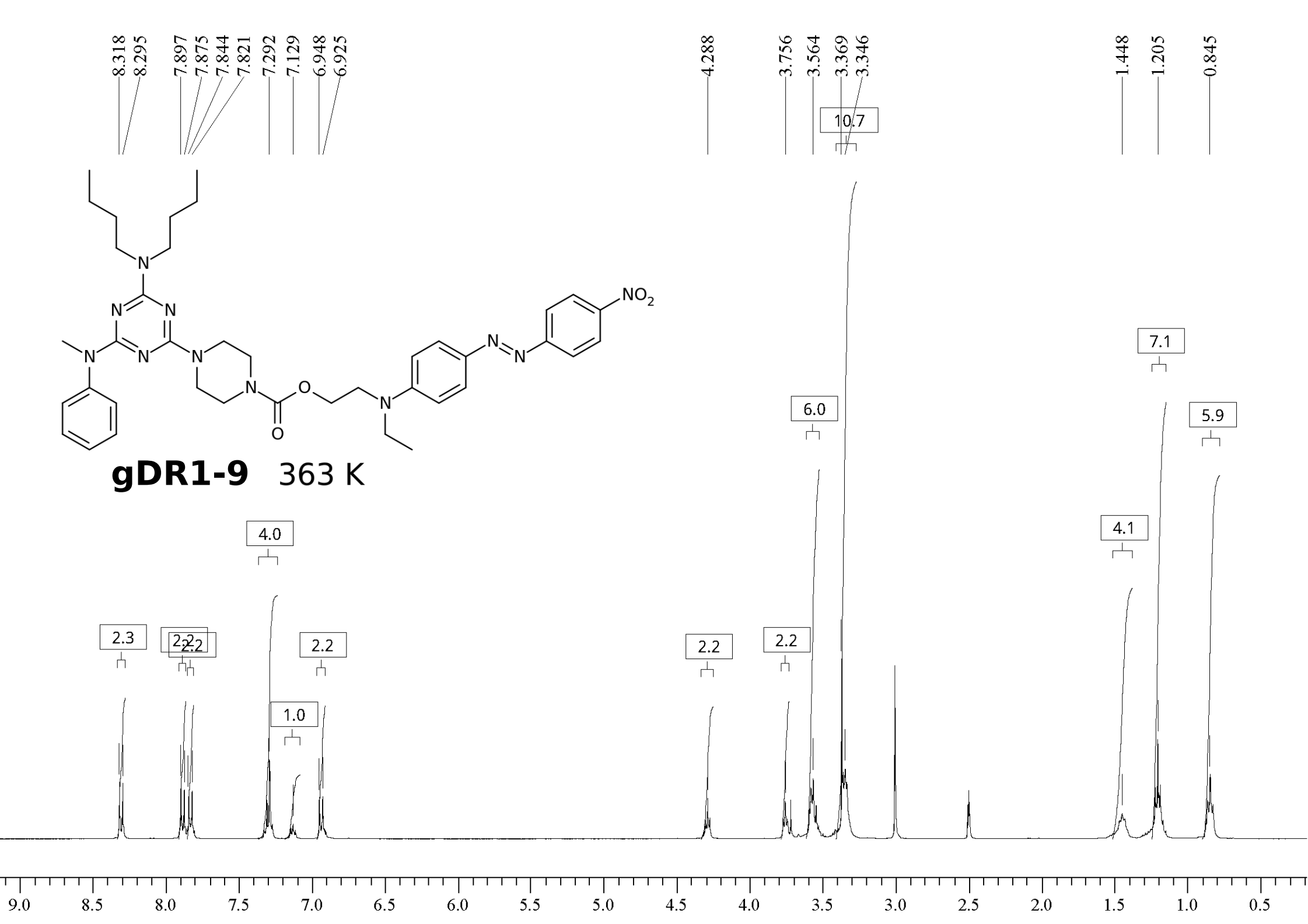
8.318
8.295
7.897
7.875
7.844
7.821
7.292
7.129
6.948
6.925
4.288
3.756
3.564
3.369
3.346
1.448
1.205
0.845
10.7
NO2
gDR1-9 363 K
4.0
2.3
2.2
2.2
2.2
1.0
2.2
2.2
6.0
4.1
7.1
5.9
9.0
8.5
8.0
7.5
7.0
6.5
6.0
5.5
5.0
4.5
4.0
3.5
3.0
2.5
2.0
1.5
1.0
0.5

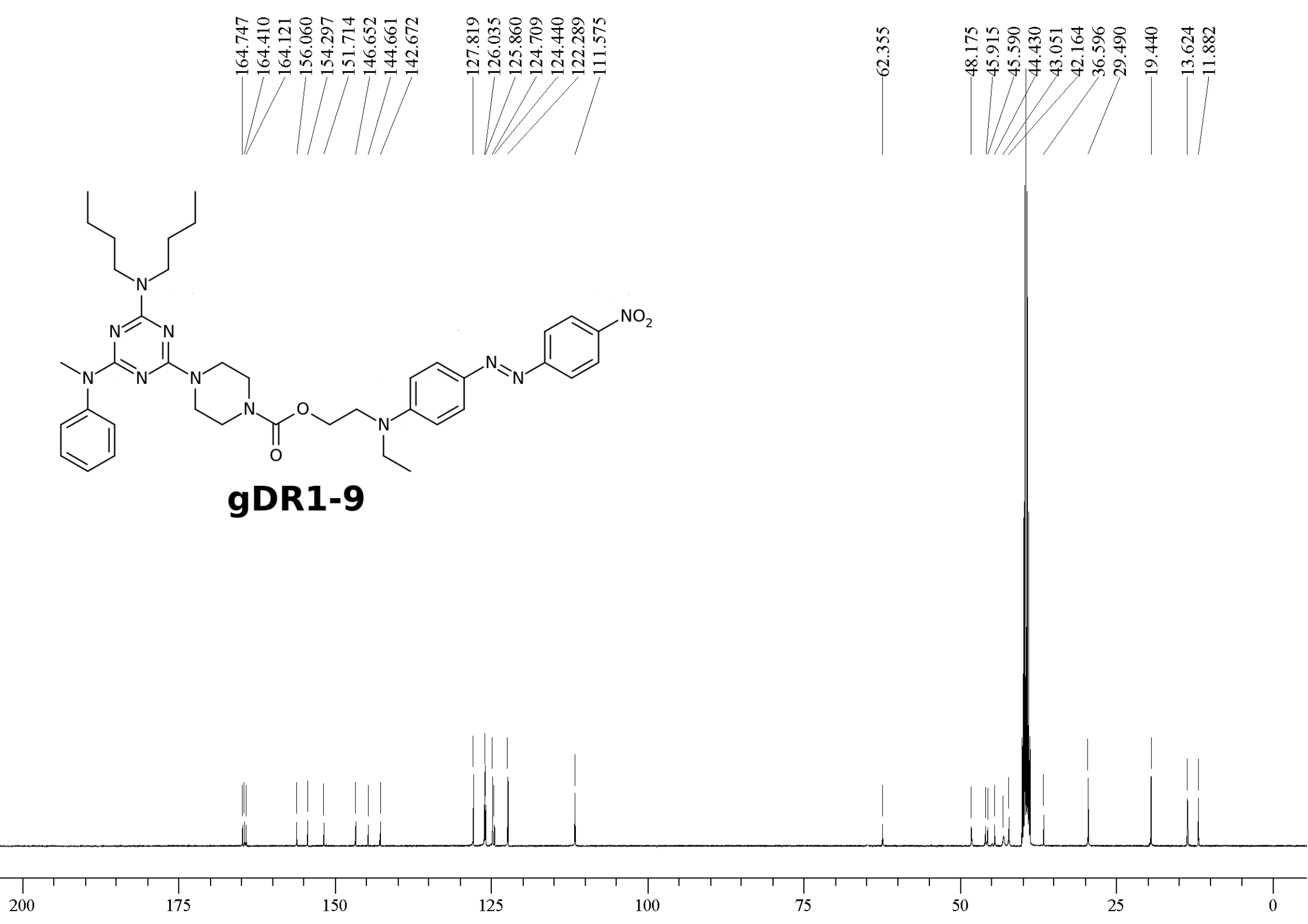
164.747
164.410
164.121
156.060
154.297
151.714
146.652
144.661
142.672
127.819
126.035
125.860
124.709
124.440
122.289
111.575
62.355
48.175
45.915
45.590
44.430
43.051
42.164
36.596
29.490
19.440
13.624
11.882
NO2
gDR1-9
200
175
150
125
100
75
50
25
0

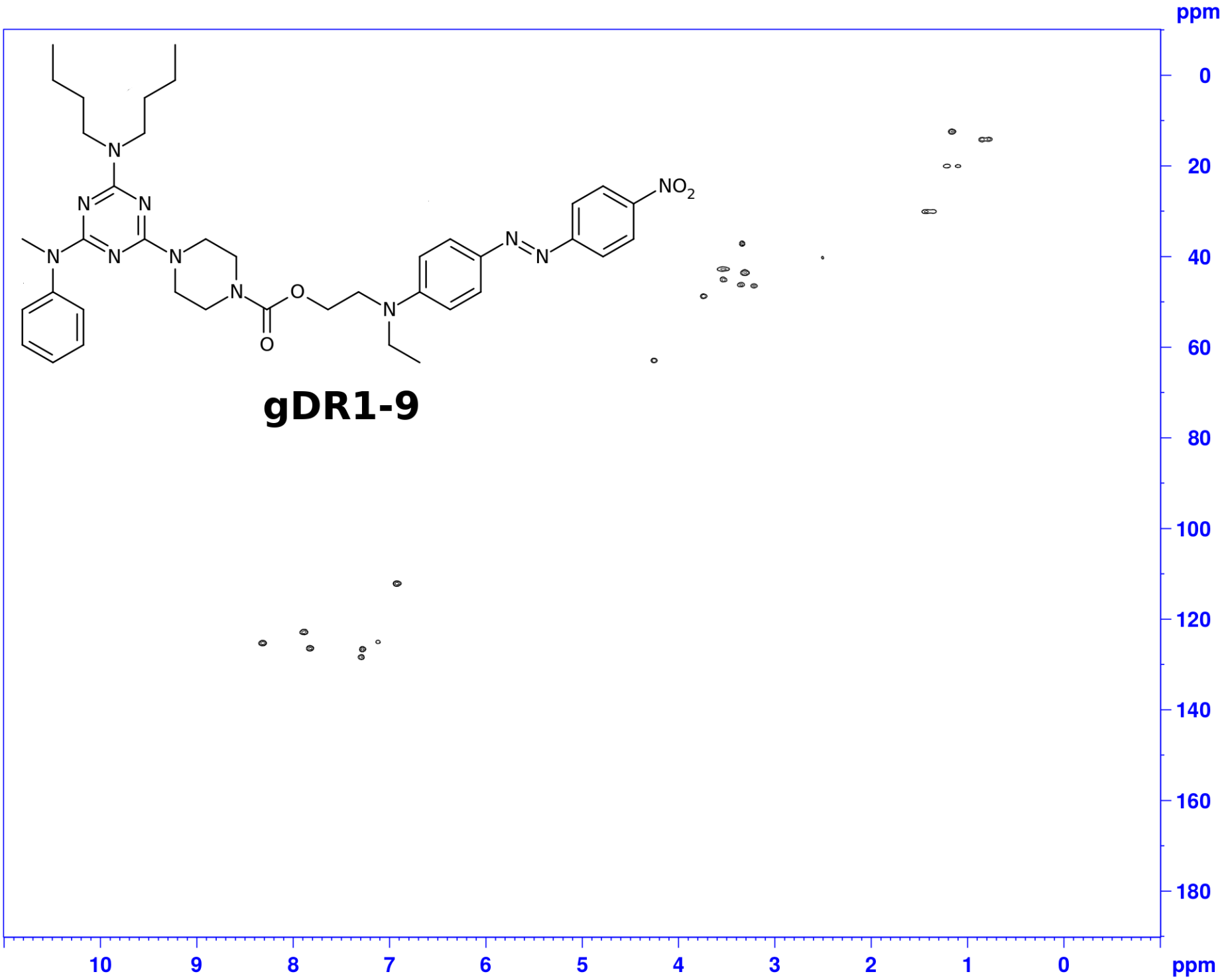
ppm
0
20
40
60
80
100
120
140
160
180
10
9
8
7
6
5
4
3
2
1
0
ppm
NO2
gDR1-9

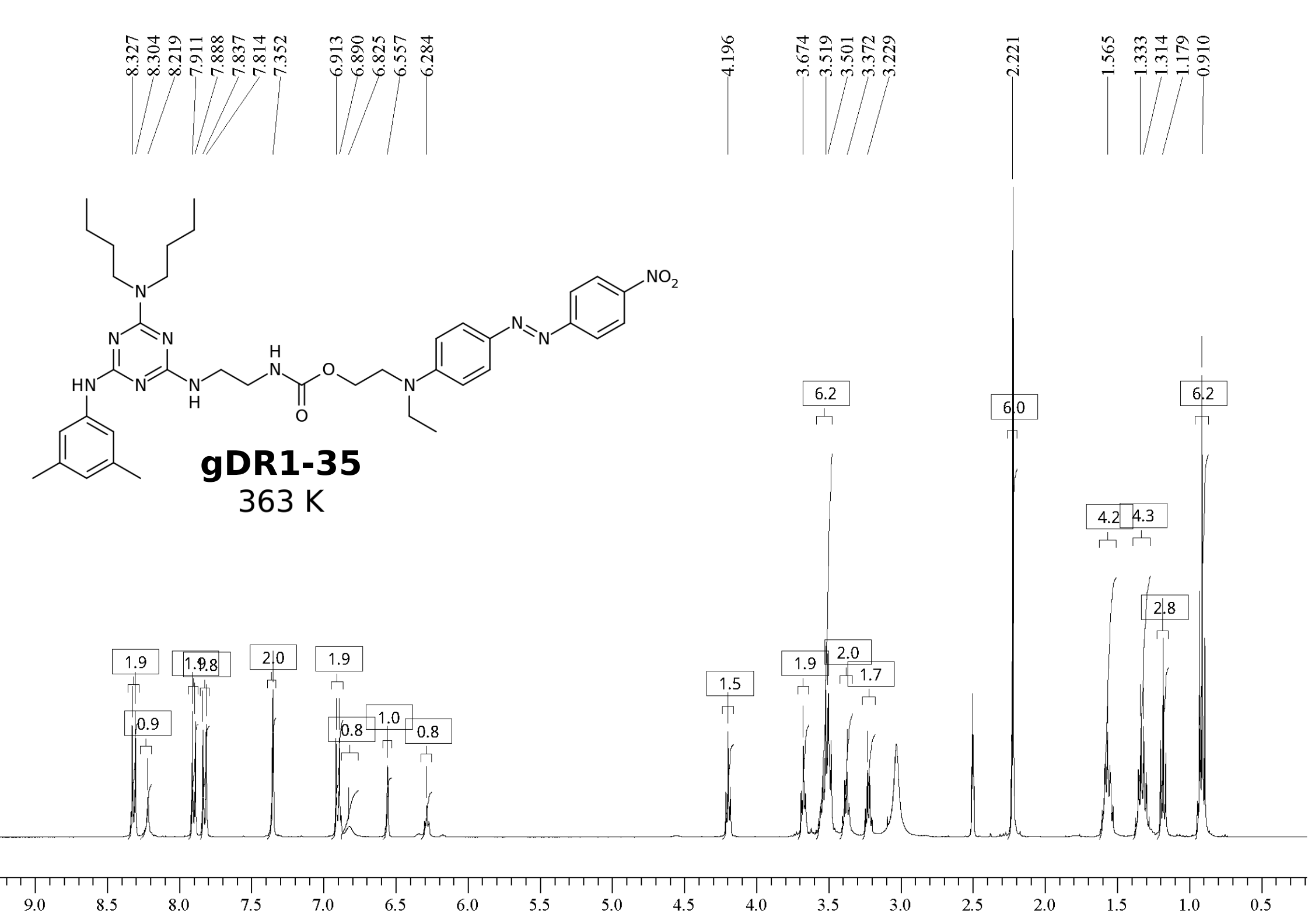
8.327
8.304
8.219
7.911
7.888
7.837
7.814
7.352
6.913
6.890
6.825
6.557
6.284
4.196
3.674
3.519
3.501
3.372
3.229
2.221
1.565
1.333
1.314
1.179
0.910
NO2
gDR1-35
363 K
1.9
0.9
1.9
1.8
2.0
1.9
0.8
1.0
0.8
1.5
1.9
2.0
1.7
6.2
6.0
6.2
4.2
4.3
2.8
9.0
8.5
8.0
7.5
7.0
6.5
6.0
5.5
5.0
4.5
4.0
3.5
3.0
2.5
2.0
1.5
1.0
0.5

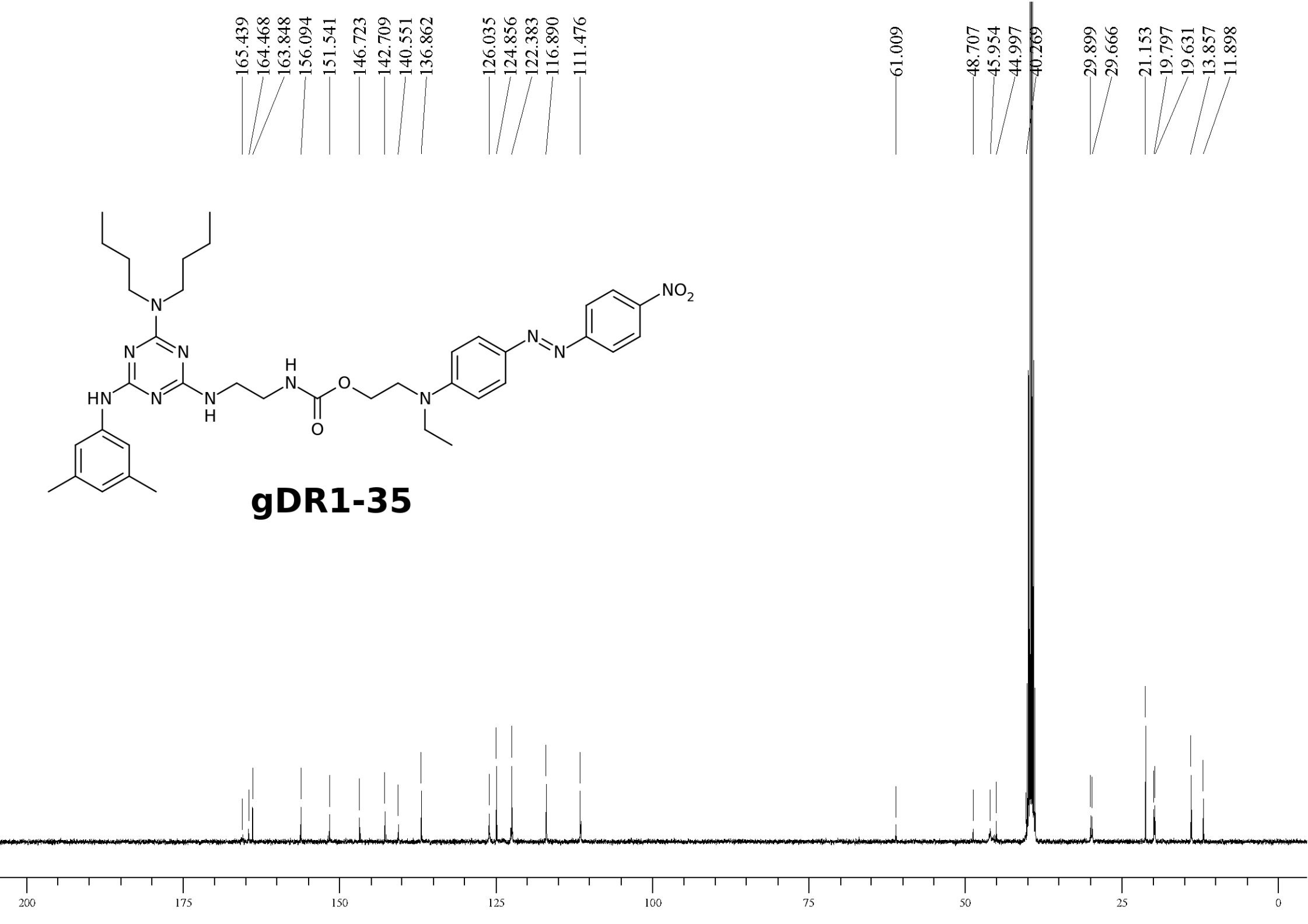
165.439
164.468
163.848
156.094
151.541
146.723
142.709
140.551
136.862
126.035
124.856
122.383
116.890
111.476
61.009
48.707
45.954
44.997
40.269
29.899
29.666
21.153
19.797
19.631
13.857
11.898
NO2
gDR1-35
200
175
150
125
100
75
50
25
0

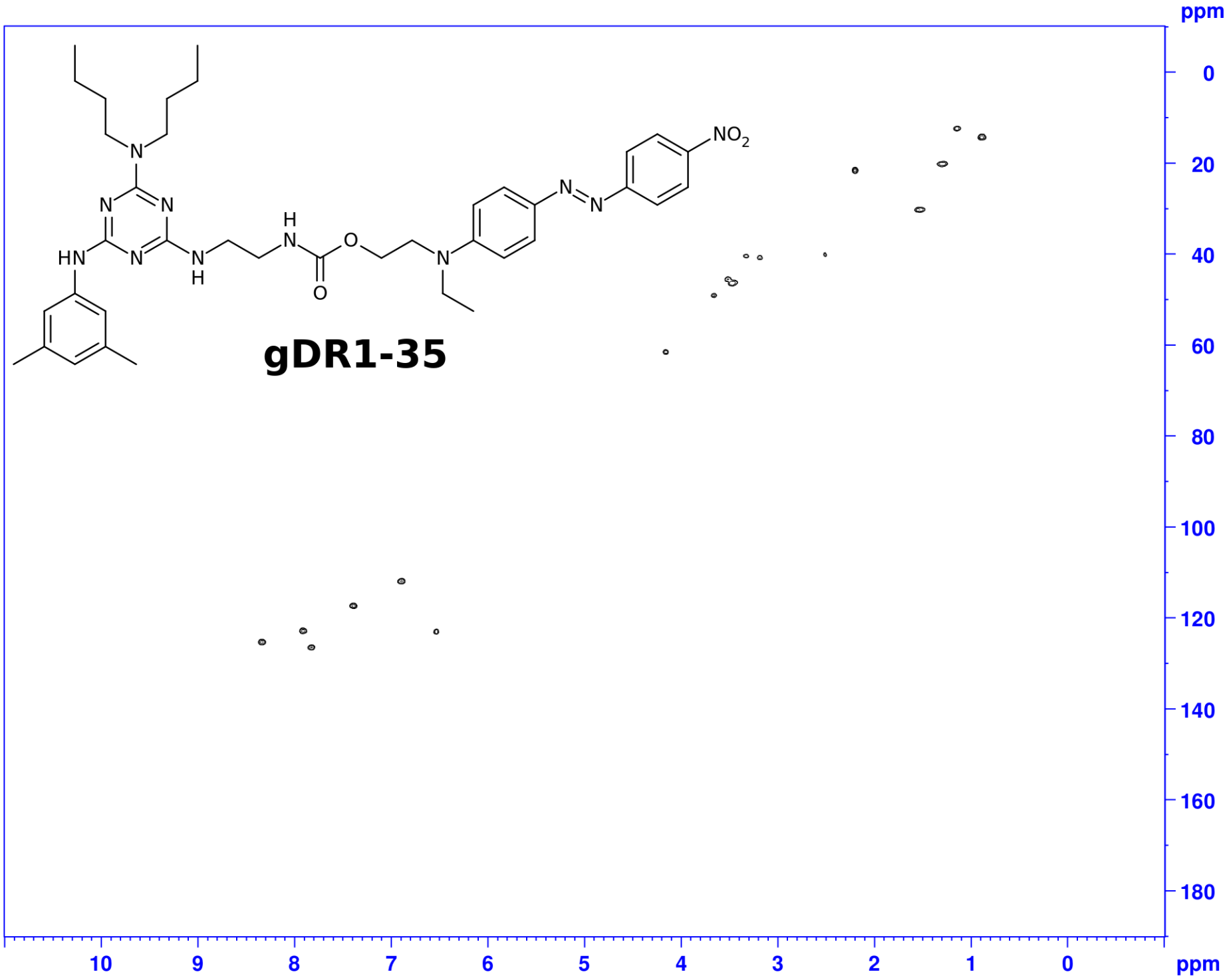
ppm
0
20
40
60
80
100
120
140
160
180
10
9
8
7
6
5
4
3
2
1
0
ppm
gDR1-35

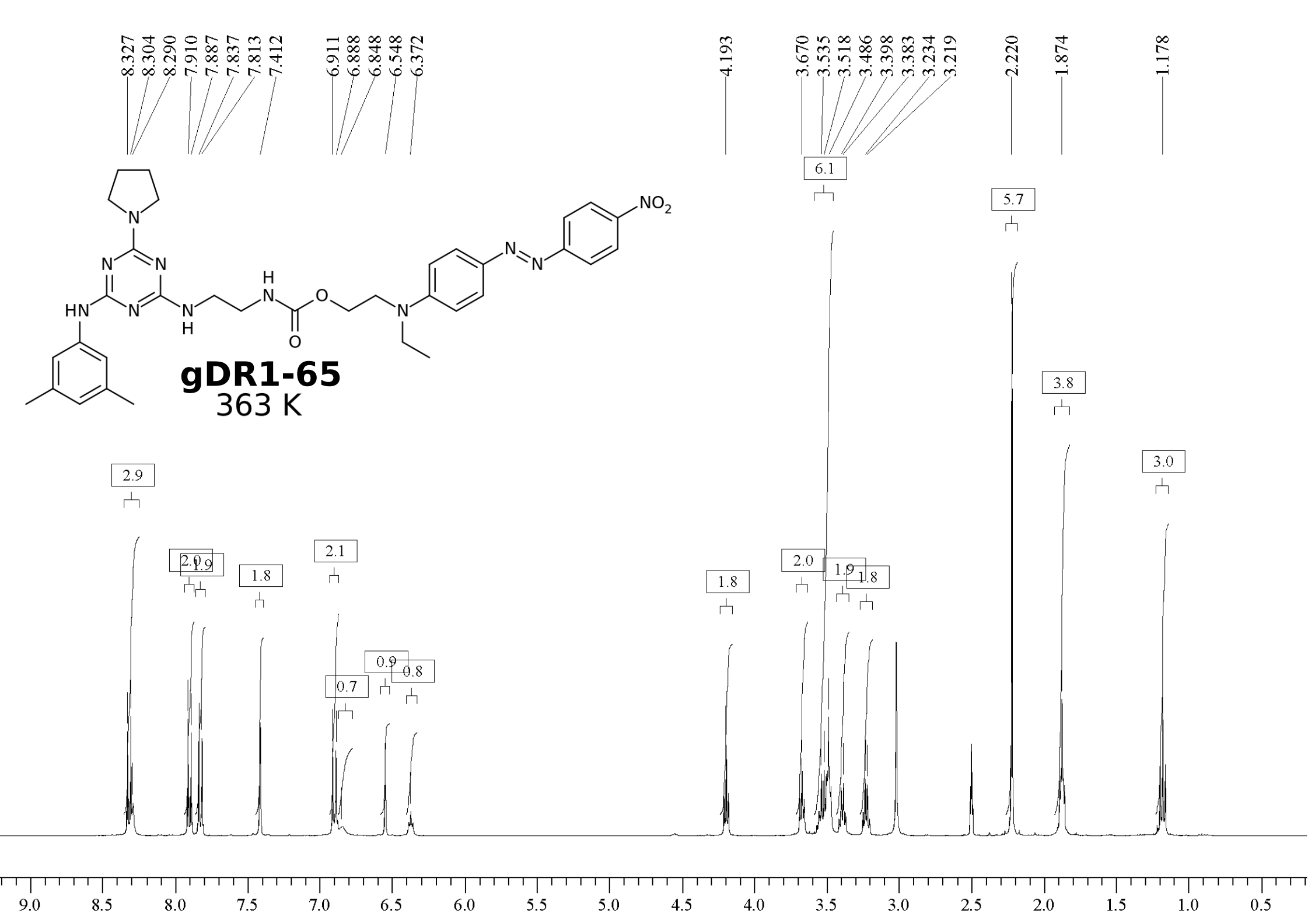
8.327
8.304
8.290
7.910
7.887
7.837
7.813
7.412
6.911
6.888
6.848
6.548
6.372
4.193
3.670
3.535
3.518
3.486
3.398
3.383
3.234
3.219
2.220
1.874
1.178
NO2
gDR1-65
363 K
6.1
5.7
3.8
3.0
2.9
2.0
1.9
1.8
2.1
0.9
0.8
0.7
1.8
2.0
1.9
1.8
9.0
8.5
8.0
7.5
7.0
6.5
6.0
5.5
5.0
4.5
4.0
3.5
3.0
2.5
2.0
1.5
1.0
0.5

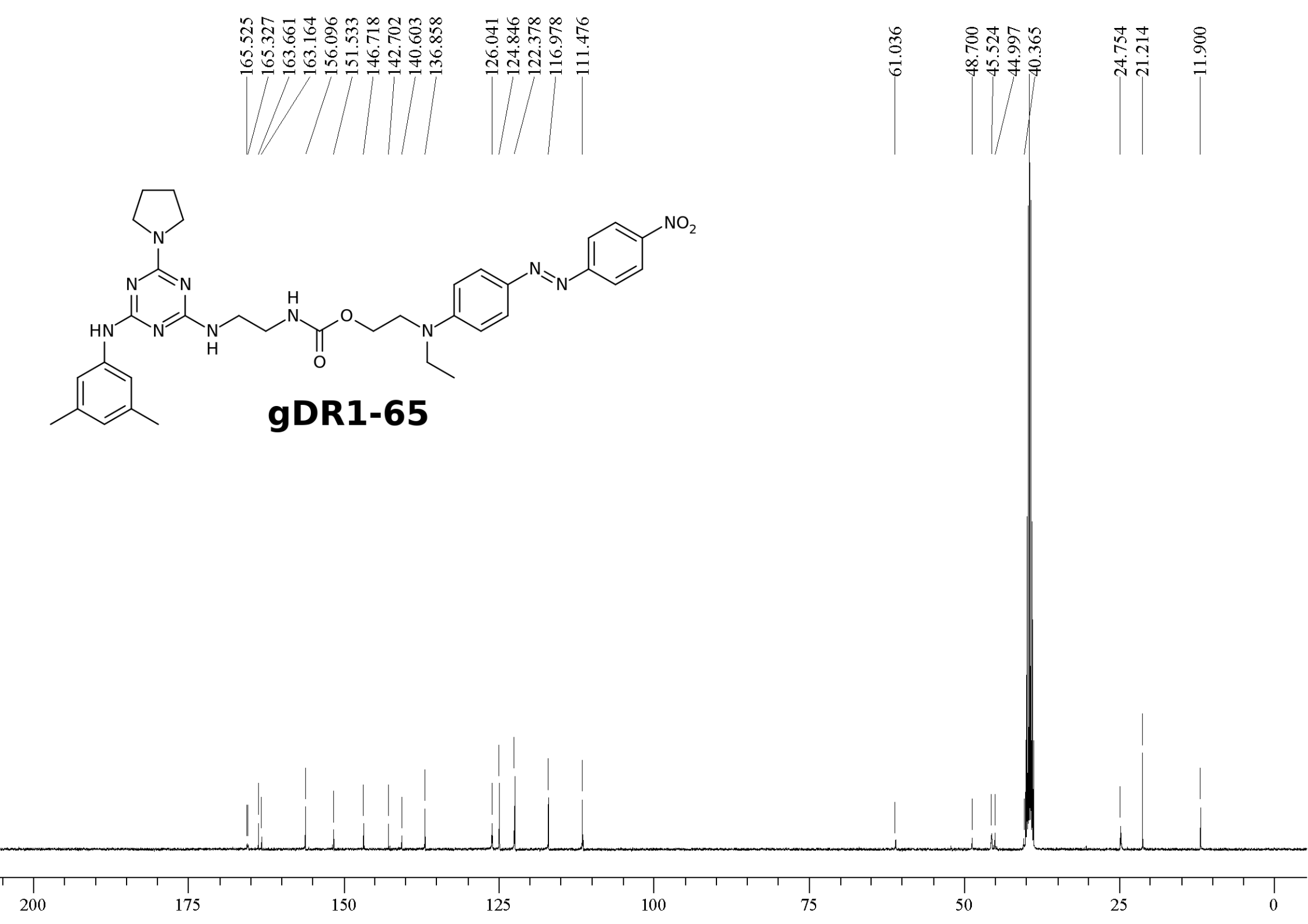
165.525
165.327
163.661
163.164
156.096
151.533
146.718
142.702
140.603
136.858
126.041
124.846
122.378
116.978
111.476
61.036
48.700
45.524
44.997
40.365
24.754
21.214
11.900
NO2
gDR1-65
200
175
150
125
100
75
50
25
0

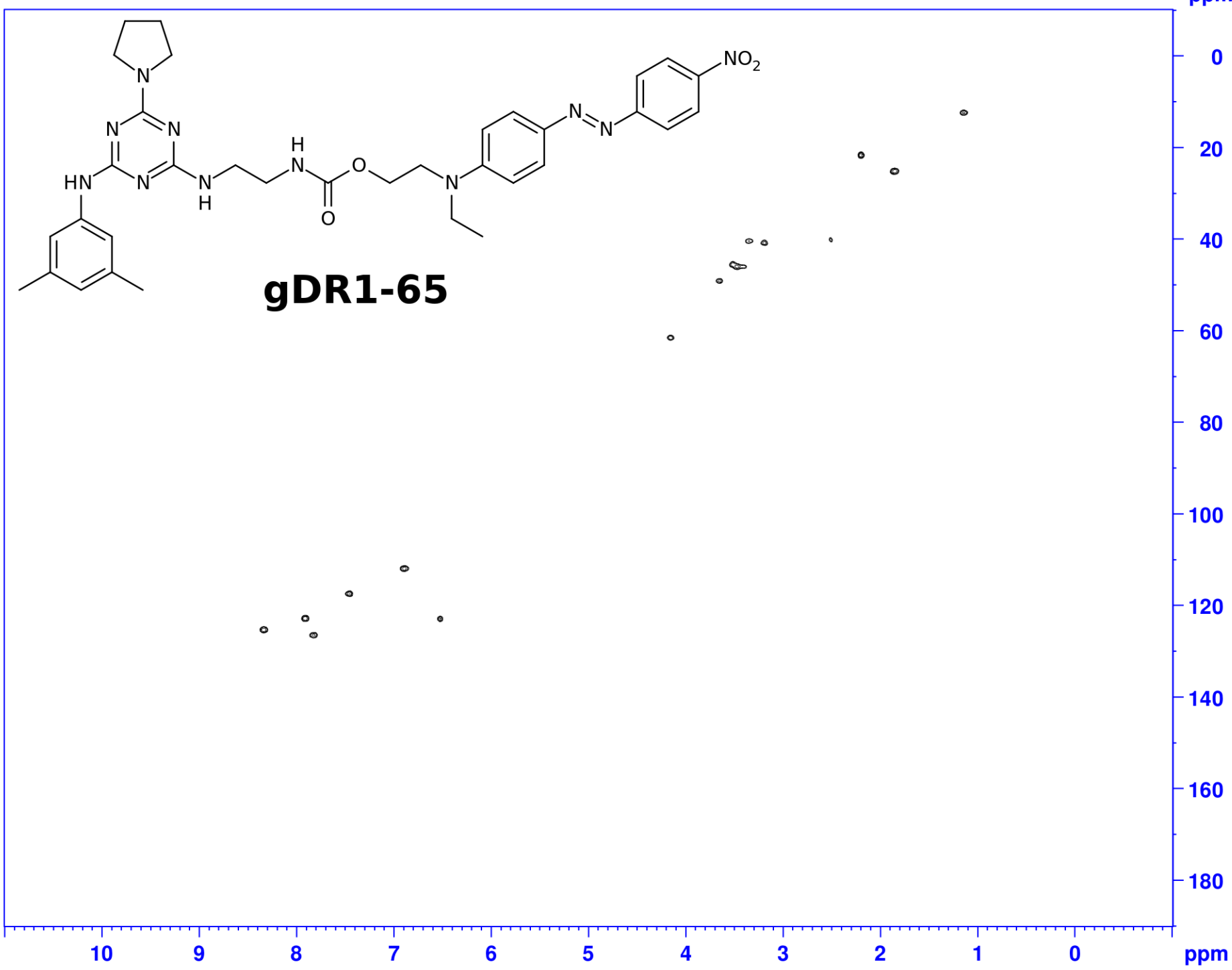
ppm
0
20
40
60
80
100
120
140
160
180
10
9
8
7
6
5
4
3
2
1
0
ppm
gDR1-65